Signature: © Pol J Radiol, 2016; 81: 401-406
DOI: 10.12659/PJR.897289

Polish Journal of Radiology
www.PolRadiol.com
CASE REPORT

Received: 2015.12.27
Accepted: 2016.01.25
Published: 2016.08.27

Authors' Contribution:
A Study Design
B Data Collection
C Statistical Analysis
D Data Interpretation
E Manuscript Preparation
F Literature Search
G Funds Collection

CT and MRI Findings in a Rare Case of Renal Primitive Neuroectodermal Tumor

Zehra Akkaya[1ABCDEF], Elif Peker[1ABCDEF], Basak Gulpinar[1ABCDEF], Hale Karadag[2ABCDEF], Ayse Erden[1ABCDEF]

[1] Department of Radiology, Ankara University, School of Medicine, Ankara, Turkey
[2] Department of Pathology, Ankara University, School of Medicine, Ankara, Turkey

Author's address: Zehra Akkaya, Department of Radiology, Ankara University, School of Medicine, Ankara, Turkey, e-mail: zehraakkaya@gmail.com

Summary

Background: Primary renal primitive neuroectodermal tumor/extraskeletal Ewing's sarcoma (PNET/EES) is a very rare renal tumor.

Case Report: We report a case of primary renal PNET/EES of the kidney in an adult patient and describe its computed tomography and magnetic resonance imaging findings, including diffusion weighted images along with a review of the current medical literature.

Conclusions: Although very rare, a relatively large renal mass which shows very infiltrative growth pattern on CT and MR imaging and striking diffusion restriction should raise the suspicion of a renal primitive neuroectodermal tumor, in a young adult.

MeSH Keywords: Diffusion Magnetic Resonance Imaging • Multidetector Computed Tomography • Neuroectodermal Tumors, Primitive, Peripheral

PDF file: http://www.polradiol.com/abstract/index/idArt/897289

Background

In recent years, with the development of imaging technologies, preoperative diagnosis of renal masses can be achieved in most cases. However, there are many overlaps with regard to the imaging findings and tissue typing is still a challenge in radiological studies. Although renal cell carcinoma is the most common primary malignant renal neoplasm and renal PNET/EES comprises only less than 1% of all adult renal tumors, it is important to diagnose PNET/EES of the kidney, which is actually a much more aggressive renal tumor of relatively younger adults [1].

Case Report

A 36-year-old male patient with a history of right-sided flank pain of two weeks' duration and a palpable flank mass was referred to our institution for further investigation after sonography in an outpatient clinic which revealed a mass. Computed tomography (CT) examination of the upper and lower abdomen was obtained with a 64-slice multidetector row scanner (Aquilion 64, Toshiba Healthcare). For CT imaging, portal venous phase images were obtained from the diaphragmatic dome to the inferior margin of the pubic symphysis with intravenous iodinated contrast material (Iomeprol 350/100 mL) at a delay of 60 seconds and a rate of 4.5 mL/s, using an automatic injection pump. The slice thickness was 1 mm and the reconstruction interval was 0.5 mm.

CT examination revealed a hypervascular, heterogeneous mass with a maximal diameter of 18 cm which compressed the inferior vena cava. The lesion was hypodense compared to renal parenchyma and it contained large central areas of cystic necrosis along with widespread internal vasculature. The central solid components were moderately enhancing relative to the periphery of the tumor (Figure 1). Metastatic lymph nodes in the retroperitoneum, including paraaortic, paracaval, interaortocaval regions have been noted. The mass showed involvement of the renal pelvis and loss of renal cortex – medulla differentiation, along with diffuse enlargement and distortion of the organ which implied the infiltrative nature of the tumor. Also CT examination revealed that the tumor had extended beyond

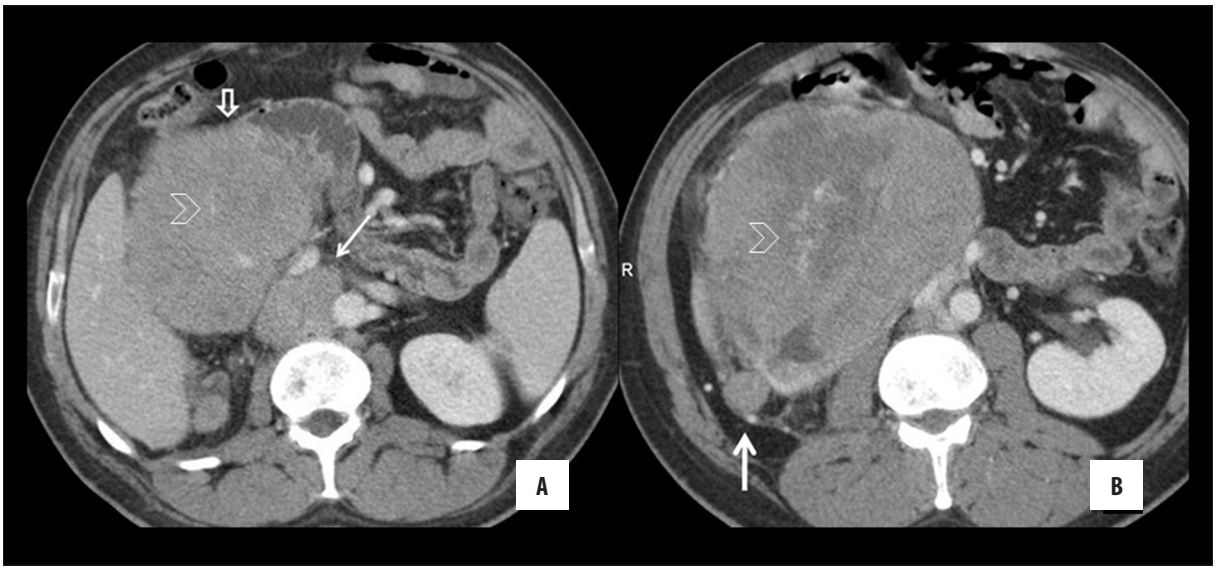

Figure 1. Axial contrast-enhanced CT image (**A**) reveals a large right-sided renal mass and interaortocaval metastatic lymph nodes (arrow). Note the small bowel invasion (open arrow) which was surgically confirmed. The linear, focal enhancing structures, (arrow heads) represent the internal vasculature of the tumor. The large mass caused severe enlargement and distortion of the right kidney (**B**) with loss of differentiation of corticomedullary ultrastructure. Note the large tumoral implant (arrow in b) in the Gerota's fascia.

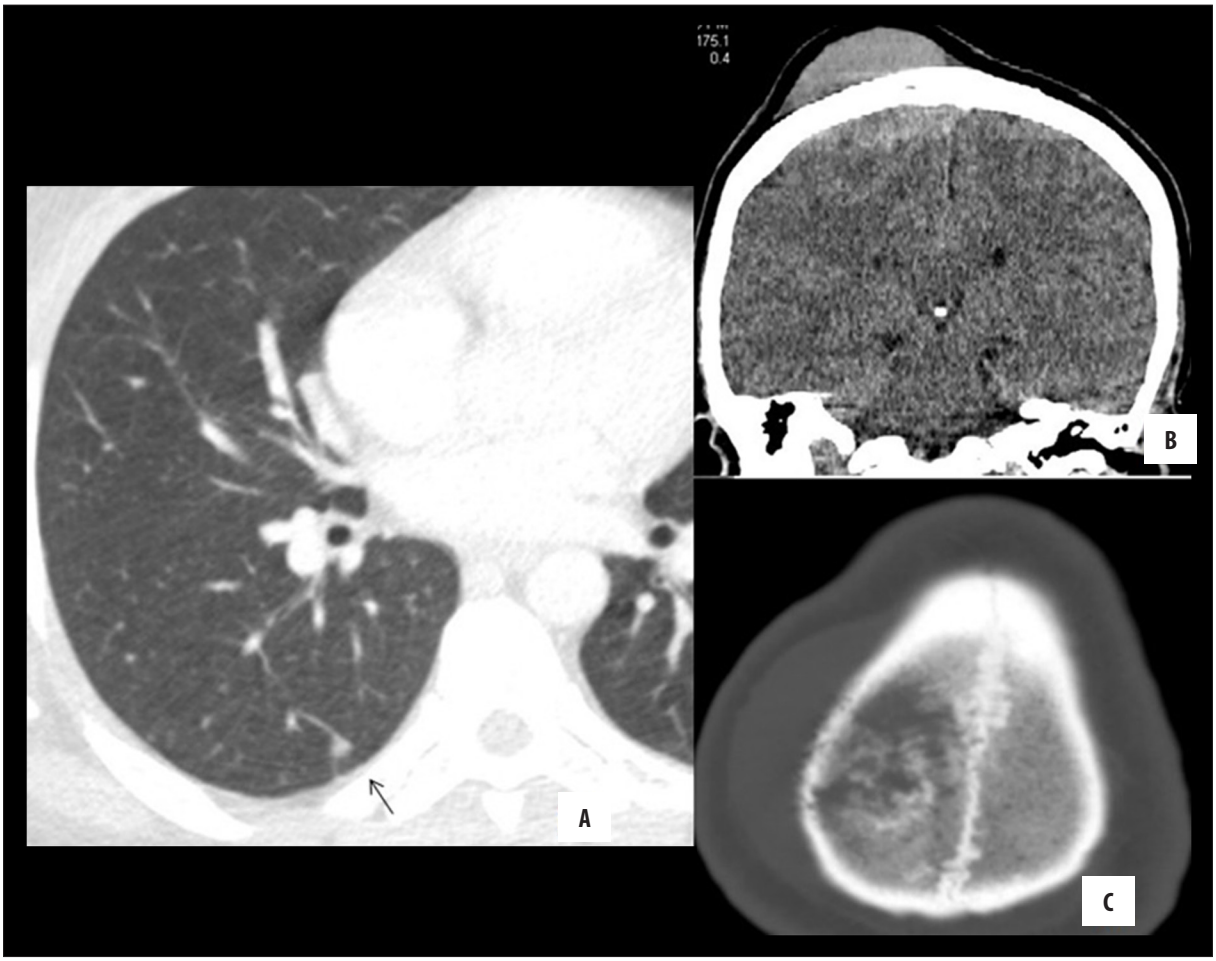

Figure 2. The chest CT image reveals a metastatic right pulmonary nodule in the right lower lobe (arrow in **A**) and soft tissue (**B**) and bone window (**C**) images of the right parietal bone metastasis are shown in cranial CT.

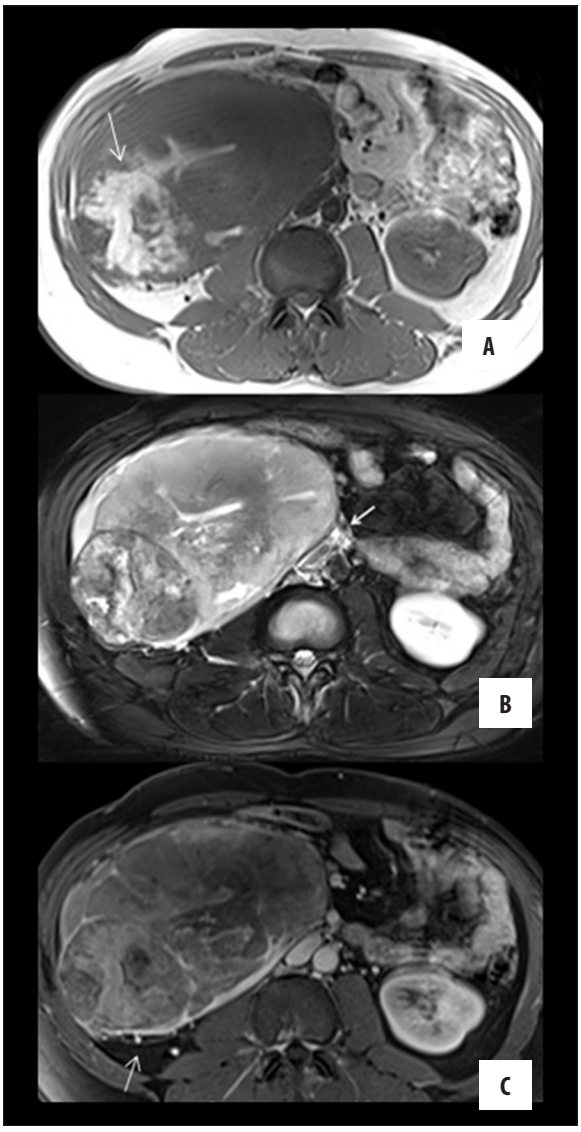

Figure 3. Axial T1-weighted (**A**), fat suppressed T2-weighted (**B**) and fat suppressed postcontrast T1-weighted (**C**) images of the tumor demonstrate its heterogeneous and hemorrhagic (arrow in **A**) content. Notice the paraaortic metastatic lymph nodes (arrow in **B**) and heterogeneous enhancement and the increased perirenal vasculature due to rich feeding vessels within the perirenal fat tissue (arrow in **C**).

the retroperitoneum and invaded a small bowel segment (Figure 1A), which was confirmed surgically. Additionally separate tumoral implants were noticed within the right perirenal tissue (Figure 1B). Metastatic lung nodules and calvarial metastasis were noticed upon further evaluation for staging of the disease (Figure 2).

Magnetic resonance imaging (MRI) study was performed on a 3T MR unit (Magnetom, Verio, Siemens Healthcare) using an 8-channel body coil.

On MRI, the hemorrhagic heterogeneous content of the tumor was readily appreciated on T1- weighted images, and the solid component appeared as hypointense to the striated muscle (Figure 3A). On T2 -weighted images the mass appeared as a heterogeneous lesion with a relatively high signal intensity (Figure 3B) and on postcontrast T1-fat suppressed images abundant feeding vessels in the perirenal fat and Gerota's fascia were seen (Figure 3C). Also the vascular displacement of the abdominal aorta and inferior vena cava was well appreciated on coronal T2-weighted (Figure 4A) and post-contrast T1-weighted images (Figure 4B).

On diffusion weighted imaging with b values 0, 400, and 1000 s/mm^2, the mass showed striking diffusion restriction with a mean ADC value of 0.64 ($\pm$0.27)$\times 10^{-3}$ mm^2/s. A similar pathologic diffusion restriction was noticed in retroperitoneal lymphadenopathy, as well as retroperitoneal tumoral implants, reflecting hypercellularity and metastatic involvement (Figures 5, 6).

The patient underwent radical nephrectomy. Renal parenchymal, pelvicalyceal and sinusal infiltration, as well as perirenal fat and Gerota's fascia invasions were confirmed in histopathological evaluation of the surgical specimen (Figure 7A, 7B). Microscopically, a small round blue cell tumor composed of small, monotonous, round cells with scant eosinophylic cytoplasms and fine granular chromatin that infiltrated the renal parenchyma were noticed. Areas of rosette formation were also suggestive of PNET (Figure 7C). Immunohistochemically, the tumor showed synaptophysin, CD 99, Fli-1 positivities and 85% proliferation index with Ki-67 (Figure 8A–8D).

On his follow-up, soon after the surgical treatment, radiotherapy and chemotherapy were started. However, the patient died within the first year after diagnosis despite aggressive treatment.

Informed consent of the next-of-kin of the patient was obtained for this article.

Discussion

PNET of the kidney belongs to small round cell tumors of the kidney which include lymphoma, clear cell sarcoma, carcinoid, monophasic Wilm's tumor, synovial sarcoma, desmoplastic small round cell tumor and extraskeletal Ewing's sarcoma (EES)/PNET [2]. Due to similar morphological and genetic characteristics, PNET and EES are considered to be virtually the same entity [3]. These tumors were first described in the literature by Mor et al. [4]. Parham et al. proposed that the origin of renal PNETs may be the adrenergic fibers which invest in the kidney from the celiac plexus or embryonal neural crest cells within the kidney [1]. As in our case, it has a predilection for male gender and in contrast to the clear cell, papillary and chromophobe types of renal cell carcinomas, it occurs more in a younger population [2]. Clinically, the most common presenting symptom is pain, followed by hematuria and renal mass [5]. Local recurrences and early metastatic disease are the causes of poor prognosis. Among the sites of metastases, lungs, pleura, bones, lymph nodes and liver have been reported, together with pulmonary tumor embolism [2,6–10].

Radiological features of the tumor have been documented in various case reports as highly vascularized tumors with

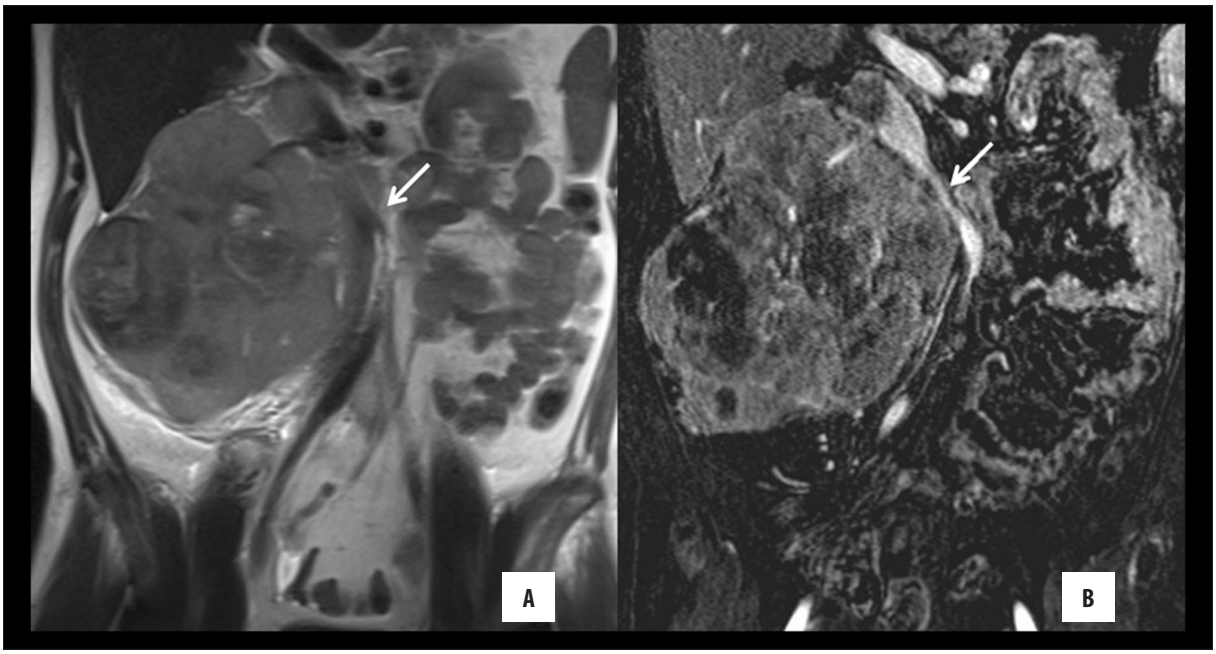

Figure 4. Coronal T2-weighted HASTE (**A**) and T1-weighted post-contrast subtraction images (**B**) showing the vascular displacement of the inferior vena cava (arrow).

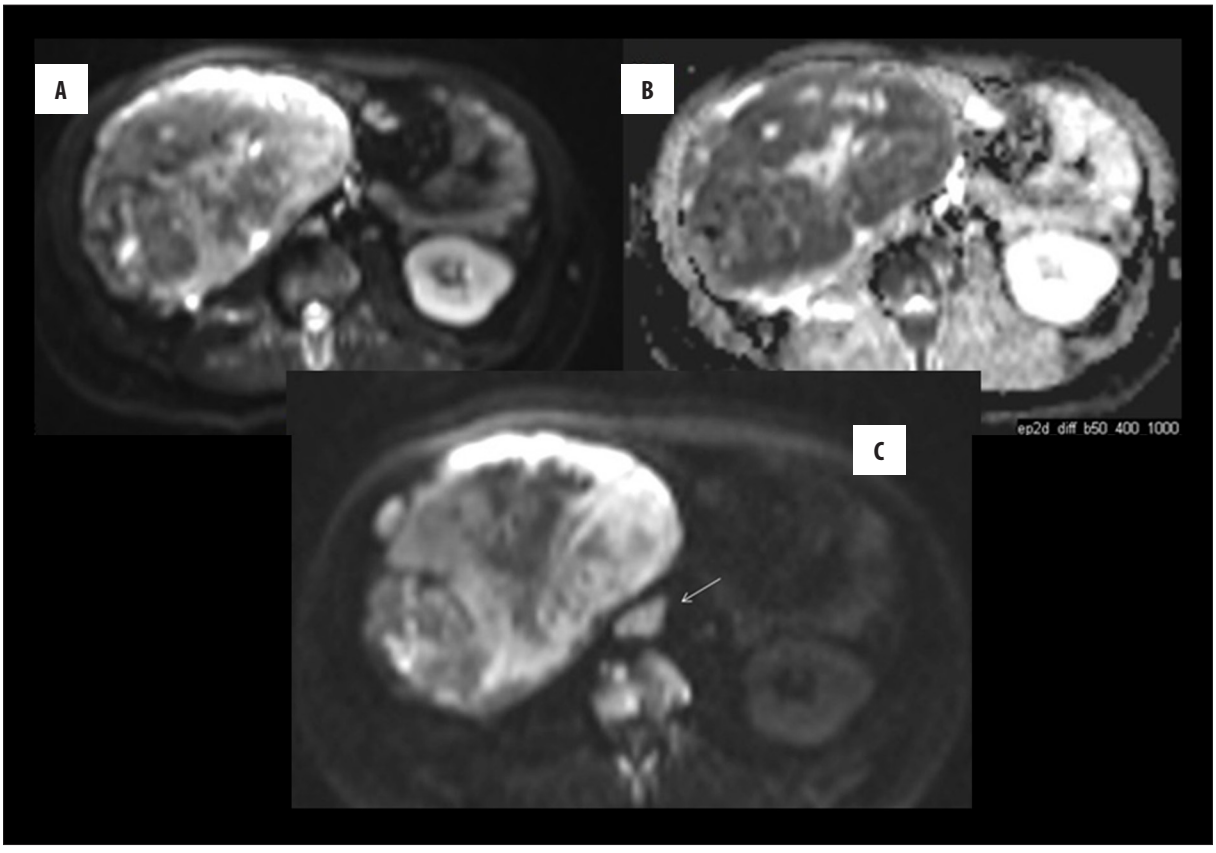

Figure 5. The mass shows marked diffusion restriction (**A, B**); notice a similar diffusion restriction in the metastatic retroperitoneal lymph node (arrow in **C**).

the diameter generally higher than 10 cm, extending into the renal pelvis therefore displacing the kidney and in some cases causing tumor thrombus in the renal vein, inferior vena cava or pulmonary arteries. [2,8]. CT characteristics were summarized as follows: solitary, large, ill-defined, irregular heterogeneous masses with invasion of the renal

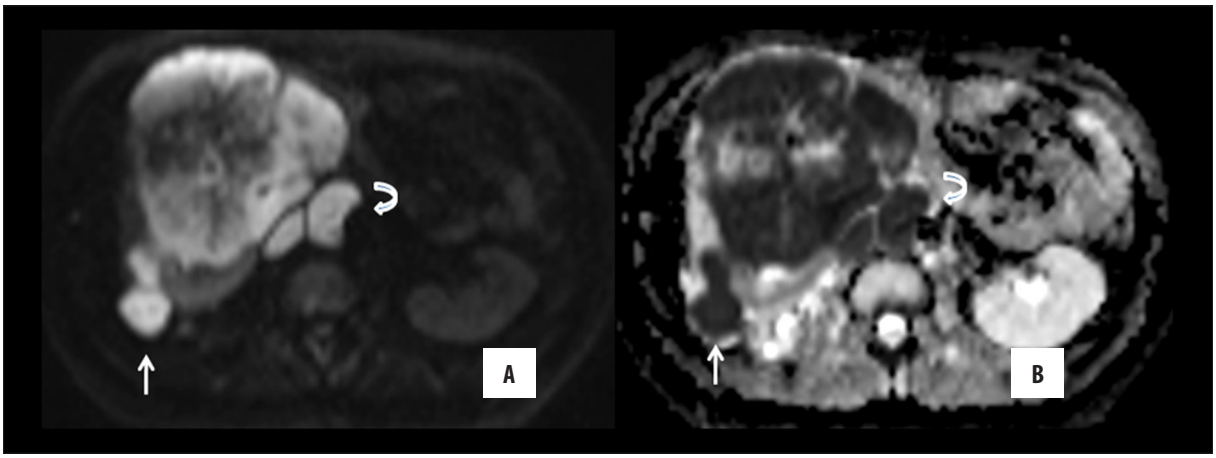

Figure 6. The diffusion weighted image with b=1000 s/mm^2 (**A**) and corresponding ADC map (**B**) of the tumor depict the significant diffusion restriction of the retroperitoneal tumoral implants (arrow) and paraaortic lymph nodes (curved arrow), as salient as the tumor itself.

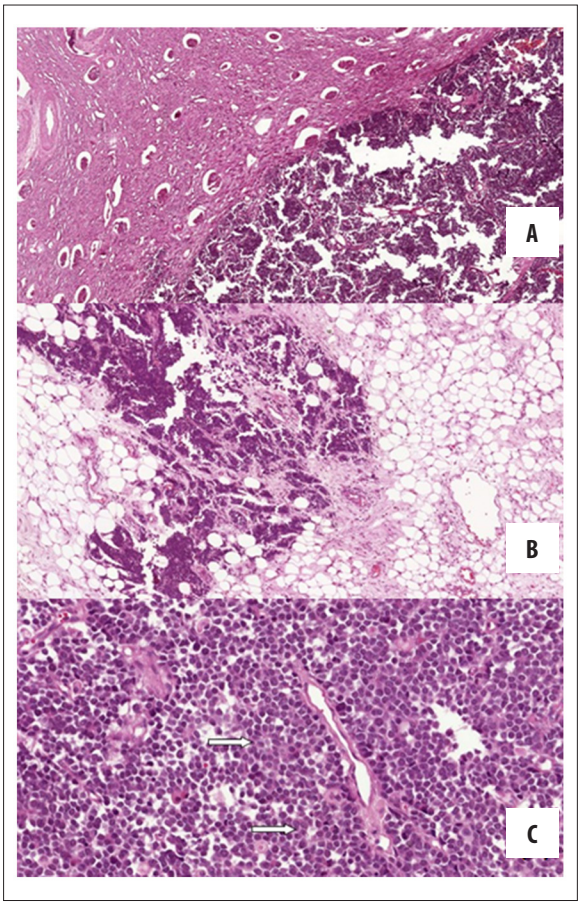

Figure 7. The tumor shows invasion of the renal parenchyma and perirenal fat (**A, B**). It is composed of uniform small round blue cells (**C**). Notice the occasional rosette formations (open arrows in **C**).

cortex and renal pelvis as well as perirenal fat and adjacent organs at the time of the initial diagnosis in most cases [6,9,11]. Lee et al. found that the enhancement of these tumors in both corticomedullary and nephrographic phases of dynamic renal CT was much lower in comparison to renal cell carcinomas [11]. Although not present in our case, fine calcification within the mass was reported in some cases at CT [12]. MRI characteristics of the tumor have been described as isointense or hypointense on T1-weighted images and heterogeneous intermediate to high signal intensity on T2- weighted images [9,10,13]. Although Zhang et al. had a case of renal PNET in their study on diffusion weighted imaging features of renal tumors, they did not specifically explain or exemplify this tumor's diffusion weighted imaging findings [14]. To the best of our knowledge, only limited case reports have been published on radiological features, especially MR imaging findings of this entity [10,13]. The diffusion restriction of the tumor is suggestive of its high cellularity and malignant nature. Although this is a single case and further studies are required, compared to the ADC values of renal carcinomas at 3T, the tumor in our case had strikingly lower ADC values [15]. We believe that this is the first report which specifies the ADC value of renal PNET.

In accordance with the previously mentioned imaging findings, our case had a relatively large infiltrative renal mass which caused distortion and enlargement of the entire organ, spread beyond the renal capsule, invaded the perirenal fat with separate tumor deposits, caused local retroperitoneal lymph node and distant organ metastases to the lungs and bones at initial diagnosis or early within the course of the disease. Although radiological and clinical features may suggest PNET in a large renal mass in a relatively young patient, definitive diagnosis requires detailed pathological examination including immunohistochemical and cytogenetical analyses [6,9].

Immunohistochemically, PNETs may express CD99, NSE, vimentin and FL-1 [7,9]. Moreover, a unique cytogenetic alteration of a reciprocal translocation t(11;22)(q24;q12) is highly specific for PNET/ Ewing's sarcoma, as it is positive in 90% of cases [1,2,8].

For treatment, surgical excision, chemotherapy and radiotherapy are required. However, despite aggressive treatment, patients with metastatic disease have poor prognosis and low overall survival rates [9].

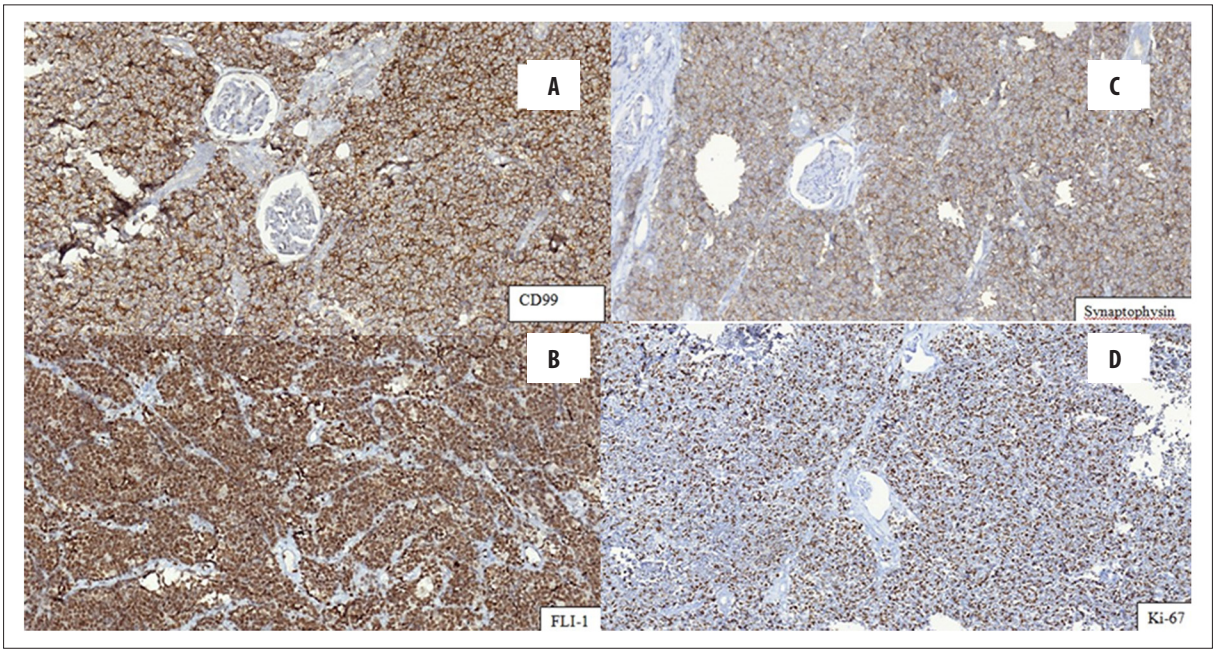

Figure 8. Immunohistochemical analysis demonstrated CD 99 (**A**), Fli-1 (**B**) and synaptophysin (**C**) positivities. Note the ubiquitous Ki-67 expression, representing the high proliferation index (**D**).

Conclusions

Despite current advances in cross-sectional imaging modalities, correct tissue typing of renal cancers, which is very important in systemic treatment options and prognosis, still constitutes a major challenge for the radiologists. Renal PNET is a very rare but significant type of kidney tumor as, unlike renal cell carcinomas, it requires early systemic treatment with chemoradiotherapy in addition to wide surgical resection. Younger age of patients and larger size than usual at presentation, early local perirenal tissue invasion, vascular invasion and/ or tumor thrombi, lymph node metastases as well as early lung and bone metastases are suggestive of a renal PNET. On imaging, large infiltrative, renal masses containing cystic- hemorrhagic areas and causing severe renal distortion with striking diffusion restriction in younger patients should alert the radiologists for this tumor.

References:

1. Parham DM, Roloson GJ, Feely M et al: Primary malignant neuroepithelial tumors of the kidney: a clinicopathologic analysis of 146 adult and pediatric cases from the National Wilms' Tumor Study Group Pathology Center. AmJ Surg Pathol, 2001; 25: 133–46
2. Businger A, Zettl A, Sonnet S et al: Primitive neuroectodermal tumor of the kidney in an adult: A case report. Cases J, 2009; 2: 6791
3. Antoneli CB, Costa CM, de Camargo B et al: Primitive neuroectodermal tumor (PNET)/extraosseous Ewing sarcoma of the kidney. Med Pediatr Oncol, 1998; 30: 303–7
4. Mor Y, Nass D, Raviv G et al: Malignant peripheral primitive neuroectodermal tumor (PNET) of the kidney. Med Pediatr Oncol, 1994; 23: 437–40
5. Risi E, Iacovelli R, Altavilla A et al: Clinical and pathological features of primary neuroectodermal tumor/Ewing sarcoma of the kidney. Urology, 2013; 82: 382–86
6. Dong J, Xing J, Limbu HH et al: CT features and pathological correlation of primitive neuroectodermal tumor of the kidney. Cell Biochem Biophys, 2015 [Epub ahead of print]
7. Jimenez RE, Folpe AL, Lapham RL et al: Primary Ewing's sarcoma/ primitive neuroectodermal tumor of the kidney: A clinicopathologic and immunohistochemical analysis of 11 cases. Am J Surg Pathol, 2002; 26: 320–27
8. Chinnaa S, Das CJ, Sharma S et al: Peripheral primitive neuroectodermal tumor of the kidney presenting with pulmonary tumor embolism: A case report. World J Radiol, 2014; 6: 846–49
9. Almeida MF, Patnana M, Korivi BR et al: Ewing sarcoma of the kidney: A rare entity. Case Rep Radiol, 2014; 2014: 283902
10. Lalwani N, Prasad SR, Vikram R et al: Pediatric and adult primary sarcomas of the kidney: a cross-sectional imaging review. Acta Radiol, 2011; 52: 448–57
11. Lee H, Cho JY, Kim SH et al: Imaging findings of primitive neuroectodermal tumors of the kidney. J Comput Assist Tomogr, 2009; 33: 882–86
12. Sharifi Doloui D, Fakharian T, Yahyavi V et al: Primitive neuroectodermal tumor with kidney involvement: A case report. Iran J Radiol, 2014; 11: 4661
13. Ekram T, Elsayes KM, Cohan RH, Francis IR: Computed tomography and magnetic resonance features of renal Ewing sarcoma. Acta Radiol, 2008; 49: 1085–90
14. Zhang J, Tehrani YM, Wang L et al: Renal masses: Characterization with diffusion – weighted MR imaging – a preliminary experience. Radiology, 2008; 247: 458–64 [published erratum appears in Radiology]
15. Goya C, Hamidi C, Bozkurt Y et al: The role of apparent diffusion coefficient quantification in differentiating benign and malignant renal masses by 3 Tesla magnetic resonance imaging. Balkan Med J, 2015; 32: 273–78